High content analysis of γ-secretase activity reveals variable dominance of presenilin mutations linked to familial Alzheimer's disease

Cristina Florean [a,b], Enrico Zampese [a], Marion Zanese [b,c], Lucia Brunello [a], François Ichas [b,c], Francesca De Giorgi [b,c], Paola Pizzo [a,*]

[a] Department Biomedical Sciences and CNR Institute of Neuroscience, University of Padua, Via G. Colombo, 3, 35121 Padua, Italy
[b] INSERM U916, VINCO, Institut Bergonié, 229 cours de l'Argonne, 33076 Bordeaux, France
[c] FLUOFARMA, 2 rue Robert Escarpit, 33600 Pessac, France

ARTICLE INFO

ABSTRACT

γ-Secretase mediates the intramembranous proteolysis of amyloid precursor protein (APP), Notch and other cellular substrates and is considered a prime pharmacological target in the development of therapeutics for Alzheimer's disease (AD). We describe here an efficient, new, simple, sensitive and rapid assay to quantify γ-secretase activity in living cells by flow cytometry using two membrane-bound fluorescent probes, APP-GFP or C99-GFP, as substrates for γ-secretase. The principle of the assay is based on the fact that the soluble intracellular domain of GFP-tagged APP (AICD-GFP) is released from the membrane into the cytosol following γ-secretase cleavage. Using this feature, enzymatic activity of γ-secretase could be deduced from the extent of the membrane retention of the probe observed after plasma membrane permeabilization and washout of the cleaved fraction. By applying two well-known γ-secretase inhibitors (DAPT and L-685,458), we validated our assay showing that the positional GFP-based probes for γ-secretase activity behave properly when expressed in different cell lines, providing the basis for the further development of a high-throughput and high content screening for AD targeted drug discovery. Moreover, by co-expression of different familial AD-linked mutated forms of presenilin – the key component of the γ-secretase complex – in cells devoid of any endogenous γ-secretase, our method allowed us to evaluate in situ the contribution of different presenilin variants to the modulation of the enzyme.

© 2008 Elsevier B.V. All rights reserved.

1. Introduction

Alzheimer's disease (AD) is characterized by the cerebral deposition of 38–42 amino acid peptides termed β-amyloid (Aβ).These result from the normal proteolytic processing of the amyloid precursor protein (APP) by β- and γ-secretases [1,2]. BACE1, a transmembrane aspartyl protease, is the major β-secretase, which cleaves APP within the extracellular/luminal domain, releasing a large soluble fragment (sAPP-β) and leaving a 99-residue C-terminal fragment (C99-CTF) in the membrane [3]. C99 can then be further processed in situ by γ-secretase that releases the Aβ peptides and a cytoplasmic tail dubbed APP-intracellular domain (AICD). γ-Secretase cleaves C99 at discrete positions, generating Aβ peptides of variable length (from 38 to 42 amino acids). Although Aβ40 is the predominant species, Aβ42 aggregates at a much faster rate and at lower concentrations, and constitutes the major component of amyloid plaques diffusely deposited in the parenchyma of the AD brain [4]. Alternatively, APP can be cut, via a non-amyloidogenic pathway, by α-secretases which produce a soluble extracellular fragment, called sAPPα, and a mem-

brane associated, 83-residue C-terminal fragment called C83. This latter is then cleaved by γ-secretase to produce AICD and p3 peptide, which is not involved in amyloidogenesis [5].

AICD is reported to bind different molecules and to take part in various cellular events including APP processing and trafficking, apoptosis, neuronal growth and regulation of gene transcription [6]. Intriguingly, AICD initiates at a site that is distal to the canonical γ-cleavage site, the so-called ε-cleavage site. The latter is located between Leu-49 and Val-50 (Aβ numbering), in a region that exhibits a strong similarity with the intramembrane cleavage site of Notch, another substrate for γ-secretase (see below) [7]. In addition, a further APP cleavage site (ζ), generating the Aβ46 intermediate precursor of secreted Aβ, has been recently identified [8]. Pharmacological data indicate that γ-cleavage requires preceding ε- and ζ-cleavages, suggesting that all of these three events are catalysed by a single enzyme [9–11]. Moreover, the production of equimolar amounts of AICD and Aβ from the cleavage of APP carboxyl-terminal fragment (C99) by γ-secretase has been clearly established [12], reinforcing the idea of a single enzymatic activity.

γ-Secretase is a multimeric enzyme made of four transmembrane proteins: presenilin 1 (PS1) or presenilin 2 (PS2)-derived N- and C-terminal fragments (NTF and CTF), nicastrin, APH-1 (anterior pharynx defective phenotype 1), and PEN-2 (presenilin enhancer 2)

[13]. Knock-down experiments have revealed that the γ-secretase components assist each other during their biogenesis and their traffic out of the endoplasmic reticulum. All four components are required to undergo proper post-translational maturation and to achieve stability (reviewed in [14]). PS1 and PS2 are polytopic nine-pass transmembrane proteins which, as catalytic members of the γ-secretase complex, play an essential role in Aβ production [15]. Genetic mutations in the *APP*, *PSEN1*, and *PSEN2* genes are responsible for early-onset familial Alzheimer's disease (FAD) [16], all exerting their pathogenic influence by selectively elevating the levels of highly fibrillogenic Aβ42 peptides. In addition to APP proteolysis, PSs play a crucial role in the intramembrane γ-secretase cleavage of a variety of type I membrane proteins including Notch1 and homologues, Notch ligands Delta and Jagged, ErbB-4, CD44, N- and E-cadherins [15]. In addition to the growing number of γ-secretase substrates, accumulating evidence from protein interaction and loss of function studies suggest that, aside from Aβ production, PSs regulate diverse physiological functions [15].

Since the high levels of AD fibrillogenic Aβ42 peptides depend on γ-secretase activity, potent enzyme inhibitors have been identified by screening drug libraries or by designing aspartyl protease transition-state analogues based on the APP substrate cleavage site [17]. However, most of these compounds are not specific for γ-secretase cleavage of APP and inhibit also the processing of the other γ-secretase substrates, such as Notch [18]. The lack of specificity of these molecules limits their application as possible drugs in AD therapy and prompts the scientific community to develop new methods useful for the screening of a number of candidate compounds on a large scale, able to evaluate specific enzyme activity on different substrates.

Here we describe the development of an efficient and quantitative high content assay for γ-secretase activity in live cells, directed towards either APP or Notch, designed to identify endogenous regulators, as well as new candidate inhibitor compounds, by means of high-throughput screening. The use of a cell-based assay for γ-secretase activity allows the identification of inhibitors that interact directly with the enzyme as well as compounds that impact upstream of enzyme activation. By validating our assay, we show that different FAD-linked PS mutants behave, dependently on specific substrate, as "loss of function" mutations for γ-secretase activity. Moreover, when co-expressed with their wild type counterparts, they differently keep their dominant-negative effect on normal enzymatic activity, allowing a general distinction between PS1 and PS2 FAD-linked mutations that could influence the overall diverse phenotypes characterizing the two forms of the disease.

2. Materials and methods

2.1. Reagents

The γ-secretase inhibitors DAPT and L-685,458 and the caspase inhibitor z-VAD were purchased from CALBIOCHEM (Merck KGaA, Darmstadt, Germany). The polyclonal anti-GFP antibody ab290 was purchased from abCAM (Cambridge Science Park, UK) and the polyclonal anti-actin antibody was from SIGMA (St. Louis, MO, USA).

2.2. Plasmids construction

The C99-GFP and APP-GFP constructs were created cloning the C99 fragment cDNA or the whole APP cDNA (kindly donated by Dr. Paul Murphy, Mayo Clinic Jacksonville) at the N-terminal of EGFP sequence in pEGFP-N1 vector (Invitrogen), using appropriate restriction sites. The mC99-GFP construct was obtained by site directed mutagenesis of C99-GFP (QuikChange Site directed mutagenesis Kit, Stratagene, La Jolla, CA) using specific primers (forward sequence GTG-GAC-GTT-GCG-GCC-GCT-GTC-ACC-CC, reverse sequence GGG-GTG-ACA-GCG-GCC-GCA-ACC-TCC-AC) in order to change Asp to Ala at aminoacidic position 86. The obtained construct was checked by sequence analysis. The NotchΔE-GFP construct was kindly provided by Dr. Oksana Berezovska (MassGeneral Institute for Neurodegenerative Disease, Harvard Medical School). The pcDNA3 constructs, as well as the pEF6/V5-His-TOPO ones, containing the cDNA encoding for different PS2 (M239I, N141I, T122R) or PS1 (A246E, H163R, P117L, L286V) mutants were created as previously described [13].

2.3. Cell lines and transfection

HeLa and SH-SY5Y cells were grown in DMEM supplemented with 10% FCS; wt or PS1/PS2-null (PS1−/−, PS2−/−) mouse embryonic fibroblasts (MEFs) were kindly provided by Dr. Bart De Strooper (Center for Human Genetics, KUL, VIB, Leuven, Belgium) and grown in DMEM/F-12 supplemented with 10% FCS. For microscopic and cytometric experiments cells were seeded respectively on 13 mm-diameter round glass coverslips or directly into 96-well plates, and allowed to grow to 80% confluence before transfection. Transfections were carried out using Lipofectamine™ 2000 (Invitrogen, Carlsbad, CA, USA) according to the manufacturer's instructions. To investigate the effect of different inhibitors, cells, 4 h after transfection, were incubated overnight with the indicated drug and then analyzed in Western blotting or flow cytometry. For stable protein expression, clones were isolated by using cloning cylinders and selection was carried out with 1 mg/ml of G418 (Promega, WI, USA).

2.4. Western blotting

HeLa and SH-SY5Y cell proteins were collected after 24 h from transfection as previously described by Giacomello et al. [20]. Immunodetection of C99-GFP, mC99-GFP and APP-GFP, as well as their metabolic products, was carried out using the polyclonal anti-GFP antibody ab290 from abCAM (Cambridge Science Park, UK). The proteins were visualized using the anti-rabbit IgG peroxidase conjugated (from Chemicon International) and the chemiluminescent reagent ECL (Amersham Biosciences, NJ, USA). To analyze probe subcellular distribution, cells were permeabilized for 3 min by 50 μM digitonin in an intracellular saline solution containing 50 μM EGTA (see below) and protease inhibitors (Roche); the supernatant was then collected (soluble fraction) and cells on the well (membrane fraction) were washed twice with PBS before being collected following the standard procedure. After protein determination, an equal amount of the two fractions were loaded for SDS-PAGE and Western blotting.

2.5. Confocal microscopy

Cells on coverslips were mounted on a thermostated (37 °C) chamber (Medical System Corp.) and placed on the stage of a confocal LSM 510 Meta system (Carl Zeiss), with a 63 oil immersion objective (NA 1.4) and illuminated at 488 nm. Cells were observed at the microscope after 4 h from transfection and followed for the indicated time or, in the case of cell permeabilization (made by bathing the cells with an intracellular saline solution containing 50 μM digitonin and 50 μM EGTA; see below), until all the cytosolic GFP fluorescence disappeared and an intracellular membrane fluorescent pattern was disclosed. Fluorescence images were acquired with a time frame indicated in each condition. Acquisition and processing of images were done using LSM image analysis software.

2.6. Flow cytometry

Transiently transfected (after 24 h) or stable expressing cells, treated or not overnight with the indicated drugs, were detached by trypsin. Half of each sample was resuspended in an extracellular saline solution (130 mM NaCl, 3.6 mM KCl, 10 mM HEPES, 2 mM NaHCO₃, 0.5 mM NaH₂PO₄, 0.5 mM MgCl₂, 1.5 mM CaCl₂, 4.5 g/l Glucose, pH 7.4) supplemented with 4% FCS and passed through the cytometer chamber to count total fluorescent cells; the other half sample was permeabilized by the addition of an intracellular saline solution (130 mM KCl, 10 mM NaCl, 20 mM HEPES, 1 mM MgSO₄, 5 mM succinate, pH 7.2) containing 50 μM digitonin, 50 μM EGTA and 4% FCS for 3 min and directly passed through the cytometer chamber to quantify the cells with a membrane-bound fluorescence. The fluorescent signal of GFP was measured in the FL1 channel (488 nm) of a flow cytometer (FACSCalibur, equipped with HTS Automated Micro-Titer Plate Acquisition BD, NJ, USA). The presented values (retention ratio) represent the ratio between the number of cells with membrane-bound GFP fluorescence after permeabilization over the number of total fluorescent cells for each condition. Data were collected in triplicate and statistical analysis was carried out by double tail Student's T test.

2.7. Apoptosis measurement

mC99-GFP transiently transfected cells (after 24 h) were treated overnight with the indicated drugs. Cells were then washed with PBS and incubated in an extracellular solution containing TMRM 200 nM and Verapamil 20 μM for 30 min at 37 °C. After incubation, cells were detached by trypsin, resuspended in the same extracellular solution supplemented with 4% FCS and passed through the cytometer chamber. Fluorescence was recorded in the FL3 channel at the wavelength of 530 nm and apoptosis was calculated as the percentage of cells without TMRM fluorescence respect to the total number of cells.

3. Results

3.1. Biochemical characterization of the recombinant GFP-based probes for γ-secretase activity

In order to set up an assay to monitor the γ-secretase activity in living cells, we tagged a known γ-secretase substrate, the APP C-terminal fragment C99, as well as APP itself, with GFP at their C-terminal ends (see Materials and methods and Fig. 1). The rationale was that the differential
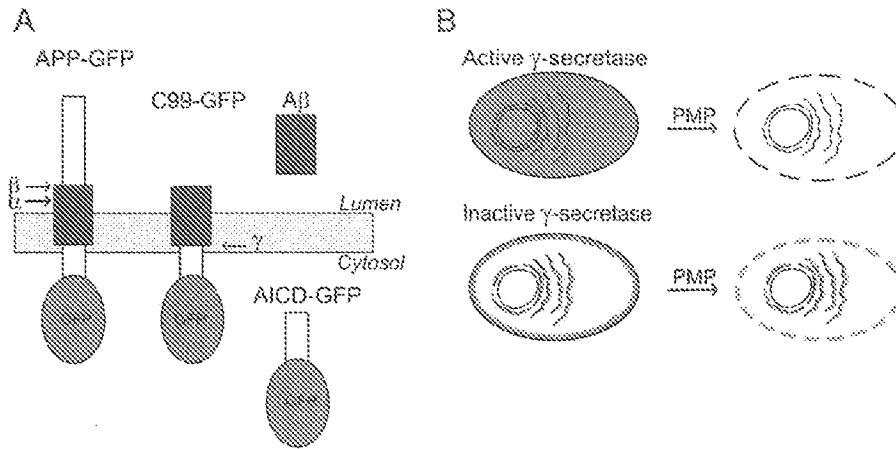
Fig. 1. Differential anchorage probes (DAPs) targeting γ-secretase activity. (A) APP and its β-secretase derived fragment, C99, were tagged with GFP at their C-terminal domain. The action of γ-secretase on C99-GFP (as well as on APP-GFP after β-secretase cutting), allows the release of Aβ in the extracellular space (or within the lumen of intracellular compartments) and AICD-GFP fragment in the cytosol. (B) Schematic representation of cell fluorescence before and after plasma membrane permeabilization (PMP) in cells with functional or inhibited γ-secretase. Only membranous fluorescence is conserved upon PMP: by comparing residual membrane-bound fluorescence with the total one, measured before permeabilization, the fluorescence retention ratio is determined, as an inverse index of γ-secretase activity.

retention of fluorescent recombinant proteins following plasma membrane permeabilization (coined "differential anchorage probes", DAPs) can be used to detect proteolytic activity: upon γ-secretase cleavage, membrane-bound C99-GFP should release Aβ into the extracellular space (or within the lumen of intracellular compartments) and AICD-GFP into the cytoplasm (Fig. 1A). By plasma membrane permeabilization, causing a loss of the soluble AICD-GFP fraction, it should thus be possible to selectively quantify the residual fluorescence

membrane retention that is a direct measurement of γ-secretase activity (Fig. 1B).

We first determined whether the two GFP constructs were good substrates for γ-secretase, as expected. HeLa and SH-SY5Y cell lines were transiently transfected with either C99-GFP or APP-GFP cDNA and treated or not with different enzyme inhibitors (Fig. 2). Western blots of control, untreated C99-GFP expressing HeLa cells show different bands (Fig. 2A, lane NT, anti-GFP antibody). By comparing this pattern with
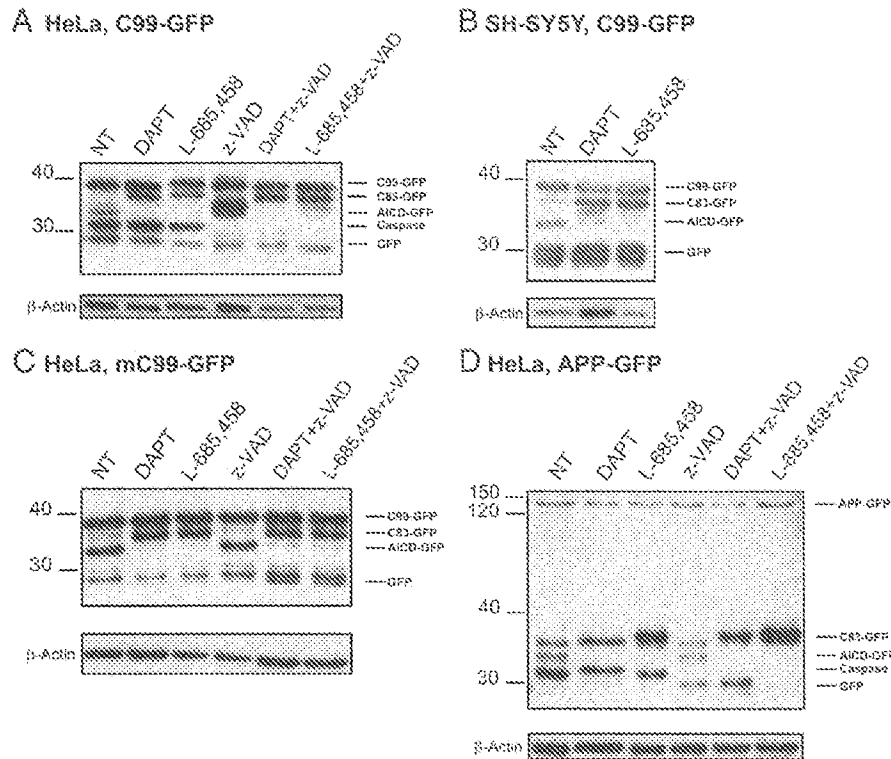

Fig. 2. Characterization of the new GFP probes cutting pattern in HeLa (A) and SH-SY5Y cells (B). Cells were transiently transfected with the GFP probe, and treated overnight with DAPT (1 μM), L-685,458 (1 μM), z-VAD (50 μM) or a combination of these drugs. Protein extracts were separated by electrophoresis, blotted and analyzed with an anti-GFP antibody. The untreated samples (NT) reveal an efficient cleavage of the probe by γ-secretase in both cell models, as demonstrated by the presence of the 35 kDa AICD-GFP band. See Results for details. (C) Protein extract from HeLa cells transfected with the mutated C99-GFP construct (mC99-GFP), lacking the consensus sequence for caspases cleavage, analyzed as in panel A. (D) Western blotting of APP-GFP transfected HeLa cells. A band corresponding to the full-length protein (APP-GFP, 137 kDa) as well as the C83-GFP, AICD-GFP and free GFP bands are shown in the untreated sample (NT). See Results for details.
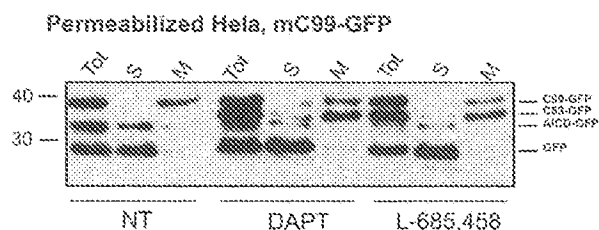
Permeabilized HeLa, mC99-GFP

Fig. 3. Differential distribution of mC99-GFP in cellular compartments upon γ-secretase activity. HeLa cells were transfected with mC99-GFP, treated overnight, or not, with DAPT (1 μM) and L-685,458 (1 μM) and then permeabilized with digitonin (50 μM, 3 min); the soluble and membranous fractions were collected separately. Total (Tot), soluble (S) or membranous (M) protein fractions were analyzed by means of Western blot with an anti-GFP antibody. Note that cell treatment with DAPT and L-685,458 changes the overall distribution of the probe, indicating that our probe works properly (see Results for detailed description).

those obtained from cells treated respectively with two well-known γ-secretase inhibitors (lanes DAPT and L-685,458), we could identify the different bands as follows: full-length C99-GFP (MW: 39 kDa), AICD-GFP γ-secretase product (strongly reduced by γ-secretase inhibitors; MW: 35 kDa), and two additional bands at minor molecular weights. The smallest one was equally present in all the lanes and corresponded to free GFP (MW: 27 kDa), probably deriving from the catabolism of C99-GFP. The remaining band corresponded to a caspase cleavage product of C99-GFP (MW: 32 kDa), since treatment with z-VAD, a pan-caspase

inhibitor, strongly reduced it. This is in agreement with the presence of a caspase cleavage site at the C-terminus of APP [21]. Interestingly, z-VAD treatment, blocking the attack of C99-GFP by caspases, favored the cleavage of C99-GFP by γ-secretase evidenced by a strong increase of the AICD-GFP band. Finally, in the DAPT and L-685,458 treated samples, a band corresponding to C83-GFP was observed (MW: 37 kDa), suggestive of α-secretase activity on C99-GFP, as previously shown [22].

Fig. 2B shows similar results for SH-SY5Y cells expressing C99-GFP: in this cell line no endogenous activity of caspases was present and the corresponding band was missing (lane NT), while γ-secretase inhibitors (lanes DAPT and L-685,458) induced the expected reduction in AICD-GFP and the appearance of C83-GFP band.

To get rid of the caspase cleavage site that interferes with our assay, we substituted the aspartic acid of the VEVD motif of C99-GFP with an alanine (VEVA; see Materials and methods). Fig. 2C shows the Western blot of HeLa cells expressing mutated C99-GFP (mC99-GFP): the caspase cleavage product has disappeared and no difference between control and z-VAD treated cells is observed (compare lanes NT and z-VAD).

Fig. 2D shows the processing of APP-GFP in HeLa cells: a higher band (MW: 137 kDa), corresponding to the full-length APP-GFP, is visible together with C83-GFP and AICD-GFP (bands increased and vanished, respectively, upon cell treatment with γ-secretase inhibitors; lanes DAPT and L-685,458); in addition, the caspase cleavage product (missing in z-VAD treated cells; lane z-VAD) and free GFP are observed. With this construct, no C99-GFP band is observed, which may suggest a preferential cleavage of APP-GFP by α-secretase. This
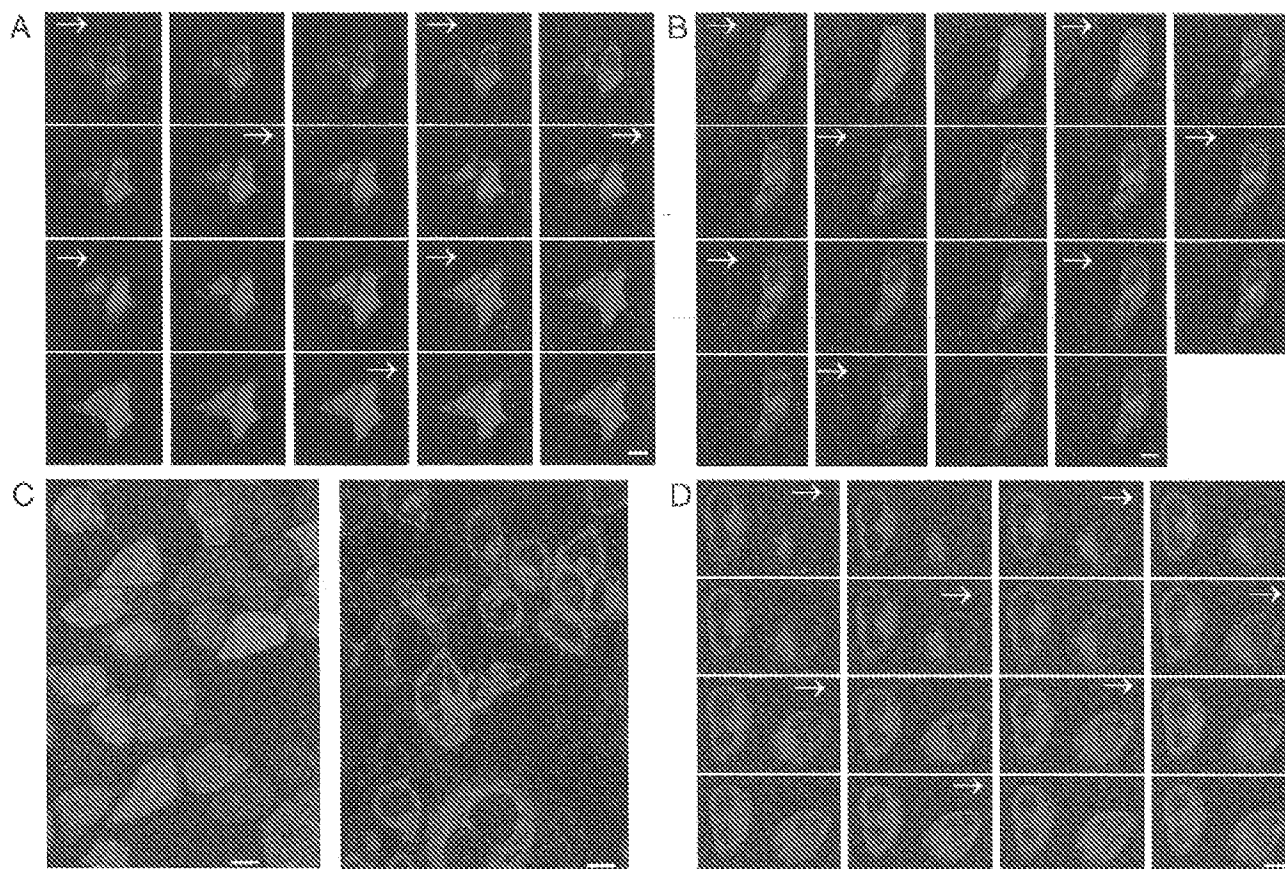

Fig. 4. Confocal images of HeLa cells expressing either mC99-GFP or APP-GFP. (A) Living HeLa cells transiently transfected with mC99-GFP were observed 4 h after transfection and followed up to 2 h. Fluorescence images were acquired every 360 s (from the first image, on the top-left of the panel, to the last one, on the bottom-right). Note the increase in cytosolic fluorescence, indicating AICD-GFP release in the cytosol upon γ-secretase activity. (B) HeLa cells transiently transfected with mC99-GFP were observed after 4 h from transfection and permeabilized by digitonin. Fluorescence images were acquired every 12 s (from the first image, on the top-left of the panel, to the last one, on the bottom-right). After few minutes all the cytosolic fluorescence is lost and a membranous staining is obtained. (C) mC99-GFP stably-expressing HeLa cells treated (on the right) or not (on the left) with DAPT (1 μM, overnight). (D) APP-GFP transiently transfected HeLa cells were observed 4 h after transfection and followed up to 1 h. Fluorescence images were acquired every 240 s (from the first image, on the top-left of the panel, to the last one, on the bottom-right) and an increasing cytosolic fluorescence during time is disclosed. Bars, 10 μM.

result is not surprising and a very low level of β-secretase cleaved APP (C99), compared to the high level of α-secretase cleaved APP (C83), was previously reported [23].

3.2. Intracellular distribution of GFP probes upon γ-secretase activity

We next analyzed the subcellular distribution (soluble/cytosolic versus membrane-bound) of the different C99-GFP products. mC99-GFP transfected HeLa cells were treated or not with the two γ-secretase inhibitors (DAPT and L-685,458) and then permeabilized with digitonin. The two resulting protein fractions (soluble and membrane-bound) were collected separately and analyzed by means of Western blotting, using an anti-GFP antibody (see Materials and methods and Fig. 3). The three main bands, i.e. C99-GFP, AICD-GFP and free GFP, observed in non permeabilized control cells (lane Tot), appear correctly sorted between soluble and membrane-bound fractions, with the C99-GFP found only in the membrane fraction (lane M) and the other two only in the soluble fraction (lane S). As expected, upon DAPT or L-685,458 treatment, while AICD-GFP production was greatly reduced, C83-GFP also appeared (lane Tot). This latter was sorted in the membrane-bound protein fraction (lane M) together with C99-GFP, indicating that our positional probe for γ-secretase activity worked properly. Similar results were obtained with HeLa cells expressing APP-GFP: all the membrane-bound APP-GFP products (i.e. APP-GFP itself and C83-GFP) were correctly distributed in the membrane fractions whereas the expected soluble forms (AICD-GFP, the caspase product and free GFP) were present in the supernatants collected after cell permeabilization (data not shown).

We then tested our probes in living cells, analyzing the kinetics of their distribution in control conditions and following DAPT treatment.

Fig. 4A shows confocal images of HeLa cells transiently expressing mC99-GFP, analyzed 4 h after transfection and followed at the microscope for up to 2 h. A diffuse cytoplasmic fluorescence that increases during time and extends to the nucleus indicates an efficient γ-secretase cleavage of mC99-GFP, due to AICD-GFP release in the cytosol. When transfected cells were permeabilized by digitonin treatment (Fig. 4B), washout of the soluble GFP fraction revealed an underlying pattern corresponding to the Golgi apparatus and other cellular membranes. A similar membrane-bound fluorescence pattern was obtained in mC99-GFP stably-expressing HeLa cells treated with DAPT: the cytosolic signal detected in untreated cells (Fig. 4C, left panel) was strongly reduced by DAPT and a membrane GFP pattern was revealed (Fig. 4C, right panel), suggesting that, when γ-secretase cannot function, C99-GFP remains membrane bound and its fluorescence marks the endocellular membranes where it resides. These data also suggest that in mC99-GFP stably-expressing HeLa cells the γ-secretase activity is high since the majority of GFP fluorescence was cytosolic under resting conditions.

The intracellular processing of APP-GFP in HeLa cells is shown in Fig. 4D: also in this case, the cytosolic fluorescence increases with time, suggesting an efficient basal cleavage of the probe by endogenous secretases.

3.3. Detecting γ-secretase activity by flow cytometry

Once demonstrated the correct behaviour of our positional probes, we quantified, by fluorescence cytometry, their membrane retention ratio. This value is the ratio between the fraction of cells exhibiting membrane-bound fluorescence resisting cell permeabilization, and the fraction of fluorescent cells, before digitonin treatment and represents an inverse index of γ-secretase activity. Fig. 5 shows this
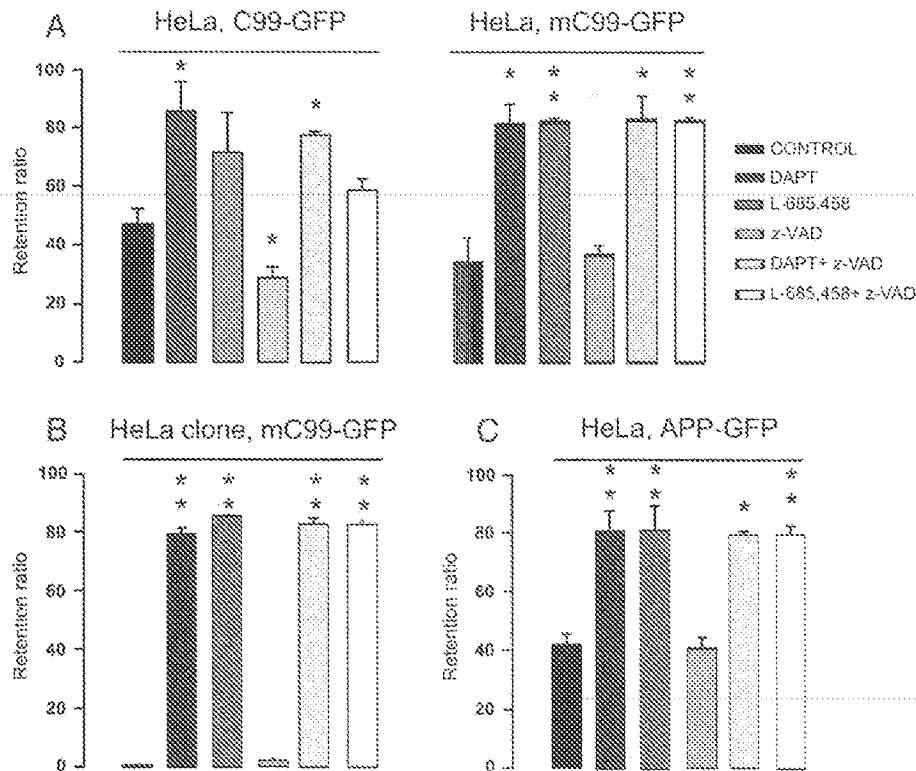

Fig. 5. Cytometric measurement of γ-secretase activity.(A) C99-GFP or mC99-GFP transiently transfected HeLa cells were treated overnight with DAPT (1 μM), L-685,458 (1 μM), z-VAD (50 μM) or a combination of these drugs. The membrane retention ratio, calculated as the number of cells with membrane-bound fluorescence after cell permeabilization, over the total fluorescent cell number before digitonin treatment, is shown as an inverse index of γ-secretase activity. (B) γ-Secretase activity detected in mC99-GFP stable expressing HeLa cells treated as in panel A. Note that inhibition of γ-secretase by DAPT or L-685,458 is almost complete in this stable cell line, as shown by a retention values over 80%. (C) Cytometric measurement of γ-secretase activity in APP-GFP transiently transfected HeLa cells. DAPT and L-685,458 treatments (as in panel A) induce a strong increase in probe membrane retention, indicating the correct behaviour of our probes. n ≥ 3; *p<0.05; **p<0.001.
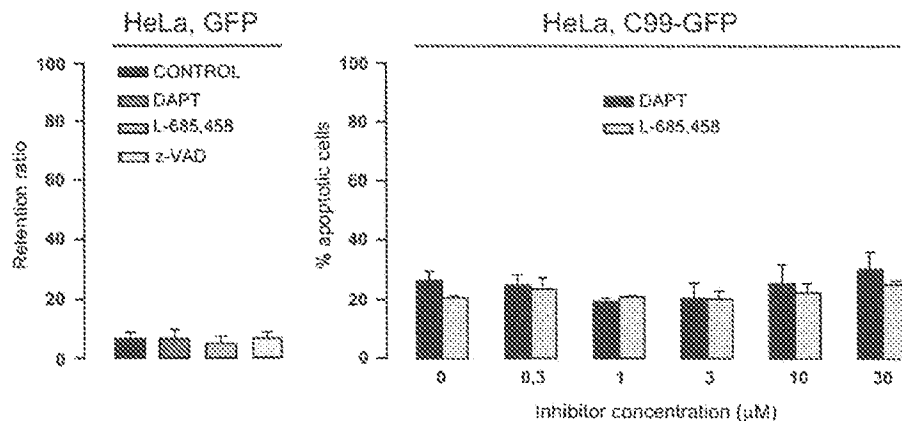
Fig. 6. Effect of γ-secretase and caspase inhibitors on GFP retention ratio and apoptosis. (A) HeLa cells transfected with GFP were treated overnight, or not, with DAPT (1 μM), L-685,458 (1 μM) and z-VAD (50 μM) and tested for membrane fluorescence retention. n≥6. (B) HeLa cells transfected with mC99-GFP were treated overnight with the indicated γ-secretase inhibitor concentrations. Apoptotic cells were counted as the number of cells lacking TMRM fluorescence over total cells in the FL3 channel (530 nm). n=3.

parameter detected in HeLa cells expressing our positional probes upon different treatments and subsequent cell permeabilization. Panel A illustrates the results obtained in transiently transfected HeLa cells with either C99-GFP (on the left) or mC99-GFP (on the right), treated or not with DAPT, L-685,458, z-VAD or a combination of these drugs. With both probes there is a similar, strong increase in membrane fluorescence retention when γ-secretase is inhibited by DAPT or L-685,458; the inhibition of caspases by z-VAD was ineffective on mC99-GFP retention, as expected, but able to weakly decrease membrane retention of C99-GFP, probably by favoring the alternative much faster γ-secretase turnover of the protein and thus rising AICD-GFP production. An unspecific effect of z-VAD, such as a variation in C99-GFP expression level or cell viability, that could explain this latter decrease in the retention ratio is unlikely since it should be found also in mC99-GFP transfected cells that instead do not show any difference in retention ratio upon this treatment (right panel of Fig. 5A).

When the cells were transiently transfected with the probes the basal fluorescence retention was estimated between 30–45% (Fig. 5A), suggesting a variability in γ-secretase activity between single cells within the population; indeed, when HeLa cells stably-expressing mC99-GFP were used for the same type of experiment (Fig. 5B), basal retention was almost negligible (≤2%) and almost complete mC99-GFP retention within cellular membranes was achieved by inhibiting γ-secretase. This result is in agreement with the confocal images (Fig. 4C) where, in untreated cells, all the GFP fluorescence was cytosolic, i.e. all the mC99-GFP was cut, but upon γ-secretase inhibition the whole probe was found to be membrane bound. Fig. 5C shows the behaviour of APP-GFP expressed in HeLa cells: also in this case, the membrane-bound fraction, measured upon γ-secretase inactivation, was markedly increased and no effect was observed upon z-VAD treatment. Similar results were obtained when the two fluorescent proteins were expressed in SH-SY5Y cells (data not shown).

In these experiments, the retention ratio of GFP alone, expressed in both cell types, was taken as a control. Noticeably, it was unaffected by all these treatments (Fig. 6A), suggesting that the different drugs were not able to unspecifically change the GFP fluorescence distribution within the cell. Moreover, none of the applied treatments appeared toxic and no cell death was induced that could have affected the readout (Fig. 6B).

Using this methodology, we estimated in live cells the half maximal inhibitory concentrations (IC$_{50}$) of DAPT and L-685,458 (Fig. 7): both γ-secretase inhibitors reached 50% of maximal fluorescence membrane retention at concentration below 0.1 μM (66 and 57 nM for DAPT and L-685,458, respectively), values very similar to those previously determined, by different methodologies, in several cell types [24–26].

3.4. Using the GFP probes, to analyze FAD-linked PSs effect on γ-secretase activity

To further validate our assay, we tested mC99-GFP metabolism in mouse embryonic fibroblasts (MEFs) either wild type (wt) or knock-out for both PS1 and PS2 (MEFs KO), the key components of the γ-secretase complex (Fig. 8). In the KO cell line no endogenous γ-secretase activity has been reported unless rescuing of the phenotype by cell expression of exogenous PSs [27,28]. In wt MEFs the retention ratio mC99-GFP was similar to that seen in HeLa cells (compare Figs. 8A and 5A) whereas in MEFs KO it was already high without any treatment and γ-secretase inhibitors were unable to affect the membrane-bound fluorescence (Fig. 8A). The lack of a complete basal retention ratio for C99-GFP in MEF KO is due to the fact that an endogenous catabolism of the expressed protein, variable in entity from cell to cell and leading to the formation of free GFP, is always present. This was checked by Western blotting in MEF KO cells transiently transfected with mC99-GFP and analyzed with an anti-GFP antibody: on the top of C99-GFP, no other cleavage product, but free GFP, was found (data not shown), supporting the fact that in these cells, where no γ-secretase activity is expected, no other enzyme is actively involved in probe cleavage.

When different PSs were transiently expressed in these cells, we could partially rescue the enzymatic activity (Fig. 8B). In particular, both wt forms of PSs (PS1 or PS2) were able to decrease the membrane-bound fluorescence (i.e. to release soluble mC99-GFP forms), while the
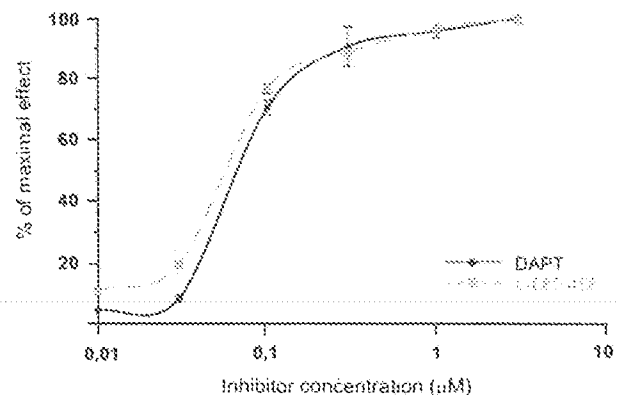

Fig. 7. Cytometric measurement of DAPT and L-685,458 half maximal inhibitory concentration (IC$_{50}$) for γ-secretase activity in stable expressing mC99-GFP HeLa cells. HeLa cells were treated overnight with the indicated drug concentration and analyzed as described in Fig. 5. For DAPT and L-685,458 an IC$_{50}$ of 66 nM and 57 nM, respectively, were determined. For each drug concentration, n=3.
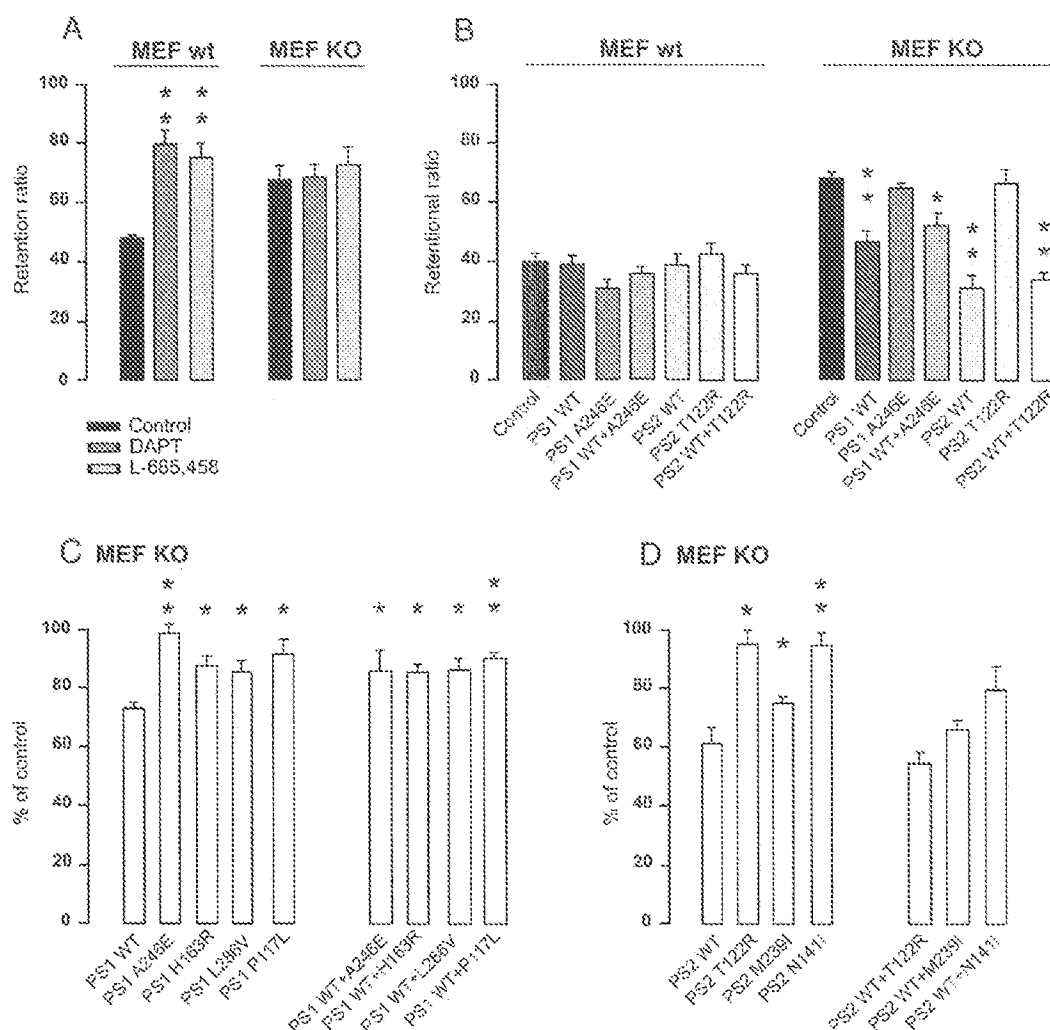
Fig. 8. Effect of specific inhibitors and FAD-linked PSs expression on γ-secretase activity in MEF cells. (A) MEFs wt or knocked-out for PS1 and PS2 (MEF KO) were transiently transfected with mC99-GFP, treated overnight with DAPT (1 μM) or L-685,458 (1 μM) and tested for fluorescence retention. Note that in MEFs KO there is no effect of γ-secretase inhibitors on probe retention ratio, which is already very high in the control condition. (B) Modulation of γ-secretase activity by PSs expression. MEFs wt or KO were transiently transfected with mC99-GFP and the indicated PS and analyzed after 24 h. Note that in MEF KO FAD-PS mutations failed to recover γ-secretase activity, acting as loss of function mutations. (C, D) MEF KO cells were transiently transfected with mC99-GFP together with one of the above reported PS forms and the cytometric assay was carried out after 24 h. $n \geq 5$; *$p < 0.05$; **$p < 0.001$.

two FAD-linked PS mutations here analyzed (PS1-A246E and PS2-T122R) behaved as loss of function mutations. The level of expression, as well as of endoproteolysis, of the different PSs was checked by Western blotting and no difference was revealed in these two parameters that could justify the lack of effect on γ-secretase activity of the mutated forms (data not shown). Moreover, when FAD-PSs were co-expressed with their wt counterparts at 1:1 ratio in MEFs KO (i.e. to mimic the pathological heterozygosis), the PS1-A246E mutant still exhibited the characteristic of a loss of function mutation, with an effect similar to that observed when expressed alone (Fig. 8B). Thus PS1-A246E exhibits a "dominant-negative" effect. In contrast, PS2-T122R, when co-expressed with PS2 wt, did not modify the retention ratio, suggesting its recessivity with respect to wt PS2. In wt MEF cells, the expression of either wt or FAD-PSs had no effect on mC99-GFP retention ratio (Fig. 8B), indicating that the presence of endogenous γ-secretase activity may likely obscure the specific effect of exogenous PSs.

To demonstrate that the difference between PS1-A246E and PS2-T122R FAD mutants in modulating the γ-secretase activity, when co-expressed with PS wt forms, is not related to the specific mutations but could be likely due to a general feature, other PS1- and PS2-FAD mutations were screened: PS1-H163R, PS1-L286V, PS1-P117L and

PS2-M239I, PS2-N141I. Strikingly, all the PS2 proteins behaved as loss of function mutants only when expressed alone; in fact co-expression of PS2 wt rescued the γ-secretase activity (Fig. 8D). In contrast, PS1-FAD forms maintained their lack of enzymatic activity even in the presence of PS1 wt, indicating their "dominance" with respect to the wt protein functionality (Fig. 8C). Thus, in heterozygosis, only PS1- but not PS2-FAD mutations were able to negatively affect γ-secretase activity.

Altogether the data here reported indicate these retention probes, used in combination with flow cytometry, as a useful and simple test for assaying γ-secretase activity in living cells. Modulation of the enzymatic activity by different compounds can be easily monitored and quantified by these probes, suggesting the feasibility of their use in a high-throughput screening approach aimed at defining new molecules as potential drugs for AD treatment. With this perspective, it is mandatory to develop a parallel assay where Notch, the other principal substrate for γ-secretase activity, is also monitored. Purposely, flow cytometric assay was carried out with HeLa, SH-SY5Y and MEF KO cells transiently transfected with the cDNA coding for the truncated form of Notch, lacking the ectodomain and fused to GFP (NotchΔE-GFP; see Materials and methods and [29]) (Fig. 9). It can be noticed that in cells with endogenous γ-secretase activity, i.e. HeLa
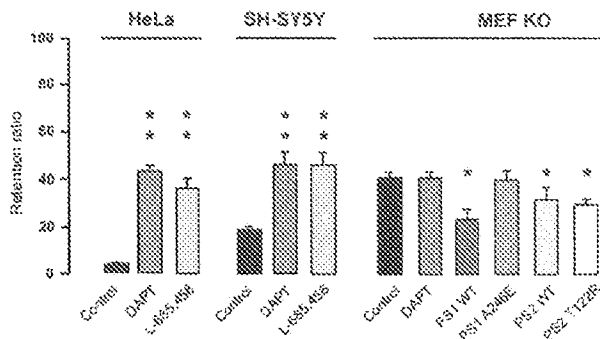
Fig. 9. Cytometric measurement of γ-secretase activity on NotchΔE-GFP: effect of inhibitors and PS expression in HeLa, SH-SY5Y and MEF KO cells. Cells, transiently transfected with the NotchΔE-GFP construct, were treated as described in Fig. 8. $n \geq 3$; *$p < 0.05$; **$p < 0.001$.

and SH-SY5Y, NotchΔE-GFP was almost completely cleaved and inhibition of the enzymatic activity by DAPT or L-685,458 led to a retention ratio of only 45% on average, suggesting possible alternative mechanisms for Notch processing. Indeed, a PS-independent Notch signaling previously reported in PS1/2 double null cells [30] has been here confirmed in MEF KO. In this cell type, lacking γ-secretase activity, the basal retention ratio was about 50%, indicating that half of NotchΔE-GFP was released from cell membranes by a different, PS-independent mechanism. In addition, when wt PS1 was expressed in these cells, an additional Notch processing was achieved. Also in the case of Notch probe, the expression of the FAD-linked PS1-A246E form determined a loss of enzymatic activity. As far as PS2 protein is concerned, two main results can be underlined. First, at variance with wt PS1 that, once expressed in MEF KO cells, recovered the γ-secretase activity by the same extent (~35%) on both mC99-GFP and NotchΔE-GFP (compare Figs. 8B and 9), wt PS2, upon expression, was less effective on NotchΔE-GFP with respect to mC99-GFP substrate (20 and 50% recovery of enzymatic activity compared to control, respectively; compare Figs. 8B and 9). Secondly, PS2-T122R did not behave as a loss of function mutation, since it acts as the wt protein when incorporated in the γ-secretase complex (Fig. 9). Thus, γ-secretase activity seems to depend on the specific molecular arrangement of the complex and shows a substrate-dependent specificity.

4. Discussion

In this study, we constructed genetically encoded GFP-based sensors that were successfully used to monitor γ-secretase activity in living cells. Our strategy consisted in the generation of retention probes capable to convert positional signals into intensity responses. The method is based on the differential retention of fluorescent recombinant proteins following plasma membrane permeabilization and is suitable for detecting a variety of molecular events, such as proteolytic activities and changes in intracellular compartmentalization [31]. We presented here specific retention probes targeting key molecular steps in a cellular pathway relevant to drug development: the γ-secretase activity.

The three membrane-bound probes used in this study (APP-GFP, C99-GFP and NotchΔE-GFP) behaved as predicted when expressed in living cells: upon γ-secretase activity they all release the soluble GFP-linked product (AICD- and NICD-GFP, respectively) in the cytoplasm allowing, upon cell permeabilization, the quantification of the residual membrane fluorescence retention that is an inverse index of γ-secretase activity. Noteworthy quantification of AICD, as a value of Aβ production by γ-secretase activity, is correct since the formation of equimolar amounts of AICD and Aβ from the cleavage of APP carboxyl-terminal fragment (C99) by γ-secretase has been clearly established [12].

The use of this assay to measure cellular γ-secretase activity has many advantages over traditional, widely used immuno-assays, such as ELISA and immunoprecipitation. Firstly, it is based on the measurement of a stable γ-secretase product, contrary to the Aβ-antibody assay that can be affected by factors modulating Aβ turnover and clearance. AICD-GFP is, in fact, very stable and easily detectable by Western blot analysis, suggesting that its catabolism by IDE [32] and/or other proteases is greatly reduced compared to unmodified AICD, as demonstrated also for other AICD-fused proteins [23]. Secondly, the genetically encoded probes are more easily obtained and cheaper than the commercial kits available for quantifying Aβ. Thirdly, the assay is particularly suited for screening of novel γ-secretase modulating drugs. The assay can be performed in a convenient 96-well microplate format using stable probe-expressing cells and can be developed for high-throughput systems. In addition, this approach allows a detailed functional characterization of drug activity directly in cells, bypassing the need for image acquisition and analysis. Thus, our retention probes constitute a robust alternative tool for high content target identification and drug discovery that could also be applied to the study of other membrane protein substrates for diverse cellular proteolytic activities [31].

Similar γ-secretase assays, alternative to the most used Aβ-antibody assays, have been previously described: all of them, however, are cell-based reporter gene assays where the γ-secretase product AICD, C-terminally tagged with Gal4/VP16, allows a Gal4-regulated reporter gene (luciferase or GFP) expression [23,33–35]. Their function depends on the responsiveness of the reporter gene and shows some disadvantages, such as background expression of the reporter gene independent of γ-secretase activity and possible interference, by different treatments, with the gene expression machinery as well as with the reporter gene product itself, as in the case of luciferase [36].

Our results show that the two recombinant probes for γ-secretase activity, mC99-GFP and APP-GFP, behave correctly when expressed in different cell types having or not endogenous γ-secretase activity (Figs. 2, 3, 4). In addition, the cytometric assay clearly measures a dose-dependent decrease in γ-secretase cleavage upon cell treatment with specific enzyme inhibitors, such as DAPT and L-685,458 (Figs. 5, 7, 8), allowing an IC_{50} determination for both inhibitors consistent with those obtained in previous reports [34–36]. Altogether these data demonstrate the specific, quantitative and sensitive functioning of our new assay for cellular γ-secretase activity readout.

To test whether the assay could identify differences in γ-secretase activity due to changes in components of the γ-secretase complex, we over-expressed wt and FAD-linked PS forms in MEF cells (Figs. 8, 9). In MEF wt cells we did not achieve any modulation of γ-secretase activity by this tool, probably due to the presence of the endogenous proteins that masks the effect of the exogenous PS forms. However, in MEF KO cells, lacking both PS1 and PS2 and thus devoid of their own γ-secretase, exogenous expression of wt PSs recovers the enzymatic function. Moreover, comparing the results from the cytometric assay carried out on both mC99-GFP and NotchΔE-GFP expressing MEF KO cells, a certain preference of PS2-containing γ-secretase complex for C99-GFP substrate was evident. Thus, it seems that, while the γ-secretase complex having PS1, as the catalytic core, cuts equally well NotchΔE-GFP and C99-GFP, PS2 expression drives a more extensive recovery of the enzymatic activity on C99-GFP compared to NotchΔE-GFP, suggesting that the PS2-containing γ-secretase complex cuts preferentially, or to a greater extent, the amyloidogenic substrate. Previous studies show that both PS1 and PS2, when expressed separately, can mediate the γ-secretase production of both AICD- and NICD-flag [37]: the relative quantification of the two cleavages was however difficult because two different antibodies were used for the detection of the specific products. Furthermore, using both an "in vitro" and a cellular assay on the C99 substrate, a different behaviour of PS1-containing γ-secretase complexes, compared to PS2-containing ones, in term of substrate specificity and

inhibitor sensitivity, was previously reported, suggesting that the two putative aspartyl class proteases may contribute to different biological processes[38]. Indeed, the diverse phenotypes exhibited by the PS1- and PS2-deficient mice may reflect these differences [39,40]. Recently, differences in specific γ-secretase inhibitor potency determinants between PS1 and PS2 sequences were reported [41], pointing out to the need of isoform specific therapeutic strategies for AD treatment. The dissimilar substrate/ligand preferences of the PS1 versus PS2 γ-secretase complex could be an important issue requiring further investigations: understanding the specificity of PS1 and PS2 toward different substrates and inhibitors will help to develop selective γ-secretase inhibitors for AD therapy. On this line, the parallel application of our cellular assay on either APP or Notch substrates, using different cell line stably-expressing PS1- or PS2-containing γ-secretase, could be very useful in a high-throughput screening approach aimed at defining new molecules with selective potency toward Aβ production and Notch signaling.

Finally, our results with FAD-linked PS expression in MEF KO cells indicate that various mutants modulate the γ-secretase activity dependently on their co-expression with the wt counterparts: in general all the FAD-PS here analyzed behave by themselves as loss of γ-secretase function mutants, as recently suggested by several authors [42–44], but only FAD-PS1 forms keep this feature when co-expressed with the wt counterpart. The different dominance on normal enzymatic activity could contribute to, or influence, the overall diverse pathogenesis characterizing the FAD PS1- or PS2-linked forms of the disease, being responsible for the more aggressive and severe phenotype of the formers.

Altogether these data suggest our positional probes as new tools for assaying the γ-secretase activity and defining the specific contribution of different isoforms, that could be part of the complex (PS1 versus PS2 or wt PSs versus FAD-linked PSs), to the enzymatic activity. In addition, modulation of the enzyme activity by different compounds could eventually be monitored and quantified, suggesting its possible use in a high-throughput screening approach aimed at defining new therapeutic strategies for AD treatment.

Acknowledgments

References

[1] D.J. Selkoe, Alzheimer's disease: genes, proteins, and therapy, Physiol. Rev. 81 (2001) 741–766.
[2] S.S. Sisodia, P.H. St George-Hyslop, g-Secretase, Notch, Ab and Alzheimer's disease: where do the presenilins fit in? Nat. Rev., Neurosci. 3 (2002) 281–290.
[3] R. Vassar, BACE1: the beta-secretase enzyme in Alzheimer's disease, J. Mol. Neurosci. 23 (2004) 105–114.
[4] D.M. Walsh, I. Klyubin, J.V. Fadeeva, M.J. Rowan, D.J. Selkoe, Amyloid-b oligomers: their production, toxicity and therapeutic inhibition, Biochem. Soc. Trans. 30 (2002) 552–557.
[5] J. Hardy, D.J. Selkoe, The amyloid hypothesis of Alzheimer's disease: progress and problems on the road to therapeutics, Science 297 (2002) 353–356.
[6] M. Raychaudhuri, D. Mukhopadhyay, AICD and its adaptors – in search of new players, J. Alzheimer's Dis. 11 (2007) 343–358.

[7] M. Sastre, H. Steiner, K. Fuchs, A. Capell, G. Multhaup, M.M. Condron, D.B. Teplow, C. Haass, Presenilin-dependent gamma-secretase processing of beta-amyloid precursor protein at a site corresponding to the S3 cleavage of Notch, EMBO Rep. 2 (2001) 835–841.
[8] G. Zhao, G. Mao, J. Tan, Y. Dong, M.Z. Cui, S.H. Kim, X. Xu, Identification of a new presenilin-dependent zeta-cleavage site within the transmembrane domain of amyloid precursor protein, J. Biol. Chem. 279 (2004) 50647–50650.
[9] G. Zhao, M.Z. Cui, G. Mao, Y. Dong, J. Tan, L. Sun, X. Xu, gamma-Cleavage is dependent on zeta-cleavage during the proteolytic processing of amyloid precursor protein within its transmembrane domain, J. Biol. Chem. 280 (2005) 37689–37697.
[10] G. Zhao, J. Tan, G. Mao, M.Z. Cui, X. Xu, The same gamma-secretase accounts for the multiple intramembrane cleavages of APP, J. Neurochem. 100 (2007) 1234–1246.
[11] Y. Dong, J. Tan, M.Z. Cui, G. Zhao, G. Mao, N. Singh, X. Xu, Calpain inhibitor MDL28170 modulates Abeta formation by inhibiting the formation of intermediate Abeta46 and protecting Abeta from degradation, FASEB J. 20 (2006) 331–333.
[12] N. Kakuda, S. Funamoto, S. Yagishita, M. Takami, S. Osawa, N. Dohmae, Y. Ihara, Equimolar production of amyloid beta-protein and amyloid precursor protein intracellular domain from beta-carboxyl-terminal fragment by gamma-secretase, J. Biol. Chem. 281 (2006) 14776–14786.
[13] T. Iwatsubo, The g-secretase complex: machinery for intramembrane proteolysis, Curr. Opin. Neurobiol. 14 (2004) 379–383.
[14] B. De Strooper, Aph-1, Pen-2, and nicastrin with presenilin generate an active gamma-secretase complex, Neuron 38 (2003) 9–12.
[15] A.L. Parks, D. Curtis, Presenilin diversifies its portfolio, Trends Genet. 23 (2007) 140–150.
[16] N. Ertekin-Taner, Genetics of Alzheimer's disease: a centennial review, Neurol. Clin. 25 (2007) 611–667 v.
[17] J. Lundkvist, J. Naslund, Gamma-secretase: a complex target for Alzheimer's disease, Curr. Opin. Pharmacol. 7 (2007) 112–118.
[18] B. De Strooper, W. Annaert, P. Cupers, P. Saftig, K. Craessaerts, J.S. Mumm, E.H. Schroeter, V. Schrijvers, M.S. Wolfe, W.J. Ray, A. Goate, R. Kopan, A presenilin-1-dependent gamma-secretase-like protease mediates release of Notch intracellular domain, Nature 398 (1999) 518–522.
[19] G. Zatti, A. Burgo, M. Giacomello, L. Barbiero, R. Ghidoni, G. Sinigaglia, C. Florean, S. Bagnoli, G. Binetti, S. Sorbi, P. Pizzo, C. Fasolato, Presenilin mutations linked to familial Alzheimer's disease reduce endoplasmic reticulum and Golgi apparatus calcium levels, Cell Calcium 39 (2006) 539–550.
[20] M. Giacomello, L. Barbiero, G. Zatti, R. Squitti, G. Binetti, T. Pozzan, C. Fasolato, R. Ghidoni, P. Pizzo, Reduction of Ca2+ stores and capacitative Ca2+ entry is associated with the familial Alzheimer's disease presenilin-2 T122R mutation and anticipates the onset of dementia, Neurobiol. Dis. 18 (2005) 638–648.
[21] E.G. Gervais, D. Xu, G.S. Robertson, J.P. Vaillancourt, Y. Zhu, J. Huang, A. LeBlanc, D. Smith, M. Rigby, M.S. Shearman, E.E. Clarke, H. Zheng, L.H. Van Der Ploeg, S.C. Ruffolo, N.A. Thornberry, S. Xanthoudakis, R.J. Zamboni, S. Roy, O.W. Nicholson, Involvement of caspases in proteolytic cleavage of Alzheimer's amyloid-beta precursor protein and amyloidogenic A beta peptide formation, Cell 97 (1999) 395–406.
[22] C. Kaether, S. Schmitt, M. Willem, C. Haass, Amyloid precursor protein and Notch intracellular domains are generated after transport of their precursors to the cell surface, Traffic 7 (2006) 408–415.
[23] C. Zhang, P.J. Khandelwal, R. Chakraborty, T.L. Cuellar, S. Sarangi, S.A. Patel, C.P. Cosentino, M. O'Connor, J.C. Lee, R.E. Tanzi, A.J. Saunders, An AICD-based functional screen to identify APP metabolism regulators, Mol Neurodegener 2 (2007) 15.
[24] H.F. Dovey, V. John, J.P. Anderson, L.Z. Chen, P. de Saint Andrieu, L.Y. Fang, S.B. Freedman, B. Folmer, E. Goldbach, E.J. Holsztynska, K.L. Hu, K.L. Johnson-Wood, S.L. Kennedy, D. Kholodenko, J.E. Knops, L.H. Latimer, M. Lee, Z. Liao, I.M. Lieberburg, R.N. Motter, L.C. Mutter, J. Nietz, K.P. Quinn, K.L. Sacchi, P.A. Seubert, G.M. Shopp, E.D. Thorsett, J.S. Tung, J. Wu, S. Yang, C.T. Yin, D.B. Schenk, P.C. May, L.D. Altstiel, M.H. Bender, L.N. Boggs, T.C. Britton, J.C. Clemens, D.L. Czilli, D.K. Dieckman-McGinty, J.J. Droste, K.S. Fuson, B.D. Gitter, P.A. Hyslop, E.M. Johnstone, W.Y. Li, S.P. Little, T.E. Mabry, F.D. Miller, J.E. Audia, Functional gamma-secretase inhibitors reduce beta-amyloid peptide levels in brain, J. Neurochem. 76 (2001) 173–181.
[25] Y. Morohashi, T. Kan, Y. Tominari, H. Fuwa, Y. Okamura, N. Watanabe, C. Sato, H. Natsugari, T. Fukuyama, T. Iwatsubo, T. Tomita, C-terminal fragment of presenilin is the molecular target of a dipeptidic gamma-secretase-specific inhibitor DAPT (N-[N-(3,5-difluorophenacetyl)-L-alanyl]-S-phenylglycine t-butyl ester), J. Biol. Chem. 281 (2006) 14670–14676.
[26] M.S. Shearman, D. Beher, E.E. Clarke, H.D. Lewis, T. Harrison, P. Hunt, A. Nadin, A.L. Smith, G. Stevenson, J.L. Castro, L-685,458, an aspartyl protease transition state mimic, is a potent inhibitor of amyloid beta-protein precursor gamma-secretase activity, Biochemistry 39 (2000) 8698–8704.
[27] A. Herreman, L. Serneels, W. Annaert, D. Collen, L. Schoonjans, B. De Strooper, Total inactivation of g-secretase activity in presenilin-deficient embryonic stem cells, Nat. Cell Biol. 2 (2000) 461–462.
[28] M. Bentahir, O. Nyabi, J. Verhamme, A. Tolia, K. Horre, J. Wiltfang, H. Esselmann, B. De Strooper, Presenilin clinical mutations can affect gamma-secretase activity by different mechanisms, J. Neurochem. 96 (2006) 732–742.
[29] C.A. Micchelli, W.P. Esler, W.T. Kimberly, C. Jack, O. Berezovska, A. Kornilova, B.T. Hyman, N. Perrimon, M.S. Wolfe, Gamma-secretase/presenilin inhibitors for Alzheimer's disease phenocopy Notch mutations in Drosophila, FASEB J. 17 (2003) 79–81.
[30] B.E. Berechid, M. Kitzmann, D.R. Foltz, A.H. Roach, D. Seiffert, L.A. Thompson, R.E. Olson, A. Bernstein, D.B. Donoviel, J.S. Nye, Identification and characterization of presenilin-independent Notch signaling, J. Biol. Chem. 277 (2002) 8154–8165.
[31] F. Ichas, F. De Giorgi, P.V. Piazza, J. Dessolin, L. Schembri, F. Tomasello, L. Lartigue, Method for demonstration of a molecular event in a cell by means of fluorescent

markers protein [French Patent No FR2857098 and World Patent Filing No WO2005/012913], (2005).

[32] D. Edbauer, M. Willem, S. Lammich, H. Steiner, C. Haass, Insulin-degrading enzyme rapidly removes the beta-amyloid precursor protein intracellular domain (AICD), J. Biol. Chem. 277 (2002) 13389–13393.

[33] H. Karlstrom, A. Bergman, U. Lendahl, J. Naslund, J. Lundkvist, A sensitive and quantitative assay for measuring cleavage of presenilin substrates, J. Biol. Chem. 277 (2002) 6763–6766.

[34] M.F. Sernee, G. Evin, J.G. Culvenor, J.A. Villadangos, K. Beyreuther, C.L. Masters, R. Cappai, Selecting cells with different Alzheimer's disease gamma-secretase activity using FACS. Differential effect on presenilin exon 9 gamma- and epsilon-cleavage, Eur. J. Biochem. 270 (2003) 495–506.

[35] Y.F. Liao, B.J. Wang, H.T. Cheng, L.H. Kuo, M.S. Wolfe, Tumor necrosis factor-alpha, interleukin-1beta, and interferon-gamma stimulate gamma-secretase-mediated cleavage of amyloid precursor protein through a JNK-dependent MAPK pathway, J. Biol. Chem. 279 (2004) 49523–49532.

[36] B.J. Deroo, T.K. Archer, Proteasome inhibitors reduce luciferase and beta-galactosidase activity in tissue culture cells, J. Biol. Chem. 277 (2002) 20120–20123.

[37] W.T. Kimberly, W.P. Esler, W. Ye, B.L. Ostaszewski, J. Gao, T. Diehl, D.J. Selkoe, M.S. Wolfe, Notch and the amyloid precursor protein are cleaved by similar gamma-secretase(s), Biochemistry 42 (2003) 137–144.

[38] M.T. Lai, E. Chen, M.C. Crouthamel, J. DiMuzio-Mower, M. Xu, Q. Huang, E. Price, R.B. Register, X.P. Shi, D.B. Donoviel, A. Bernstein, D Hazuda, S.J. Gardell, Y.M. Li, Presenilin-1 and presenilin-2 exhibit distinct yet overlapping g-secretase activities, J. Biol. Chem. 278 (2003) 22475–22481.

[39] J. Shen, R.T. Bronson, D.F. Chen, W. Xia, D.J. Selkoe, S. Tonegawa, Skeletal and CNS defects in Presenilin-1-deficient mice, Cell 89 (1997) 629–639.

[40] D.B. Donoviel, A.K. Hadjantonakis, M. Ikeda, H. Zheng, P.S. Hyslop, A. Bernstein, Mice lacking both presenilin genes exhibit early embryonic patterning defects, Genes Dev. 13 (1999) 2801–2810.

[41] B. Zhao, M. Yu, M. Neitzel, J. Marugg, J. Jagodzinski, M. Lee, K. Hu, D. Schenk, T. Yednock, G. Basi, Identification of gamma-secretase inhibitor potency determinants on Presenilin, J. Biol. Chem. 10 (2007) 1074/jbc.M708870200.

[42] J. Shen, R.J. Kelleher, The presenilin hypothesis of Alzheimer's disease: evidence for a loss-of-function pathogenic mechanism, Proc. Natl. Acad. Sci. U. S. A. 104 (2007) 403–409.

[43] M.S. Wolfe, When loss is gain: reduced presenilin proteolytic function leads to increased Abeta42/Abeta40. Talking Point on the role of presenilin mutations in Alzheimer disease, EMBO Rep. 8 (2007) 136–140.

[44] B. De Strooper, Loss-of-function presenilin mutations in Alzheimer disease. Talking Point on the role of presenilin mutations in Alzheimer disease, EMBO Rep. 8 (2007) 141–146.